Available online at www.sciencedirect.com
ScienceDirect
Journal of the European Ceramic Society 26 (2006) 3853–3859
www.elsevier.com/locate/jeurceramsoc

High strength TiC matrix Fe28Al toughened composites prepared by spontaneous melt infiltration

M.X. Gao [a,b], Y. Pan [a,*], F.J. Oliveira [b], J.L. Baptista [b], J.M. Vieira [b]

[a] *Department of Materials Science and Engineering, Zhejiang University, Hangzhou 310027, PR China*
[b] *Department of Ceramics and Glass Engineering/CICECO, University of Aveiro, Aveiro 3810-193, Portugal*

Received 27 July 2005; received in revised form 12 December 2005; accepted 6 January 2006
Available online 2 March 2006

Abstract

Fe28Al bound TiC matrix composites with TiC content of 75–90% in volume (vol.%) were successfully fabricated by spontaneous melt infiltration. Amounts of Fe28Al in excess and below the pore volume of the TiC preform were used for optimization of fabrication techniques. Young's modulus, hardness, flexural strength and fracture toughness of the composites were measured. Four-point bending strength of Fe28Al/90–75 vol.% TiC ranges to 990–1260 MPa. The high strength is attributed to the good infiltration ability of molten Fe28Al in the porous TiC preform and to processing refinements. TiC preform pre-sintering and indirect infiltration all lead to fully dense and defect-free composites. The relationship between Vickers hardness and indentation fracture toughness and the dependence of mechanical properties on microstructure of the composites were also studied. Results of SEM and XRD analysis show TiC and Fe28Al as the only crystalline phases of the composite. Fe28Al ligaments have ductile behaviour and greatly toughen the composites. Crack front deviation during fracture also increased the fracture resistance of the composites.

Keywords: Composites; Indirect infiltration; Mechanical properties; Microstructure-final; Failure analysis; Fe28Al/TiC; TiC

1. Introduction

Titanium carbide (TiC) is refractory with a high melting point (3065 °C), wear-resistance, low density (4.93 g cm^{-3}) and high hardness (20–32 GPa).[1] But monolithic TiC is brittle at room temperature. Compared to ceramics, intermetallics are ductile and tough. They also have high melting point, low density, excellent oxidation and corrosion resistance. TiC matrix composites with intermetallics as the ductile second phase are expected to yield a unique combination of properties. Fe40Al,[2,3] Ni_3Al[4,5] and NiAl[6] had been investigated for fabricating intermetallic/TiC composites by spontaneous melt infiltration. The high temperature strength of iron aluminide is lower than that of Ni_3Al, but it offers lower material cost, lower density and better oxidation and corrosion resistance in sulfidation and in molten salt environment. Values of three-point bending strength of 1050 MPa for Fe40Al/60–70 vol.% TiC and of 750 MPa for Fe40Al/80 vol.% TiC were reported by Subramanian et al.,[2,3] but for TiC content higher than 85 vol.%, defect-free composites could not be obtained. Fe40Al/TiC composites prepared by reaction sintering had limited values of three-point flexural strength of only 725 and 595 MPa for 70 and 83 vol.% of TiC, respectively.[7] Significant improvements in strength are needed for engineering applications where high strength and reliability are essential. In extending the metallic binding materials towards optimization of properties and promoting wide application of the intermetallic/ceramic composites in industry, new binding materials are required. Fe28Al, the DO_3 structured hyper-stoichiometric Fe_3Al alloy containing 28 at.% Al, excellently fits the purpose. Compared with B2 structured FeAl, Fe28Al has higher values of fracture elongation, yield strength and ultimate tensile strength than FeAl (36.5 at.% Al), both in air and in vacuum.[8,9] It is suggested that Fe28Al to be less prone to embrittlement possibly due to the lower aluminium concentration and the type of crystalline structure (i.e. DO_3 versus B2). Further, like other ordered intermetallics, Fe_3Al-based alloys also have good wear-resistance.[10]

In the present study, Fe28Al was selected as metallic binding phase to fabricate TiC matrix composites by spontaneous melt infiltration. Mechanical properties including Young's modulus,

* Corresponding author. Tel.: +86 571 8795 3008; fax: +86 571 87951152.
E-mail address: yipan@zju.edu.cn (Y. Pan).

0955-2219/$ – see front matter © 2006 Elsevier Ltd. All rights reserved.
doi:10.1016/j.jeurceramsoc.2006.01.005

flexural strength, Vickers hardness and indentation fracture toughness were measured. Improvements of mechanical reliability are estimated through the Weibull modulus. The relationship between fracture toughness and hardness and the dependence of mechanical properties on the TiC content of the composites were investigated. The fracture mechanism of Fe28Al/TiC composites was also characterized.

2. Experimental procedures

The constituent materials were TiC powder (H.C. Starck, Germany) with particle size of 1–2 μm and smelted Fe28Al intermetallic. As-received TiC powder was de-agglomerated by milling in 2-propanol with WC/Co balls then dried and sieved through a 100 mesh sieve before forming. Cuboid shaped rubber mould was filled with the TiC powder, followed by cold isostatic pressing at 200 MPa and then the TiC bars were cut and ground by sand paper to rectangular preforms of about 18 mm × 18 mm × 35 mm.

The pre-sintering of TiC preforms and the infiltration were all performed in a graphite heating furnace. The furnace chamber was evacuated to a dynamic vacuum of 10^{-2} mbar followed by letting argon flow at atmosphere pressure throughout the experiments. TiC preforms were isothermally sintered at 1500 °C × 1 h and 1500 °C × 4 h, with heating and cooling rate of all 25 °C min^{-1}, to yield preforms with relative density of 80–81% and 88–89% of the theoretical density of TiC, 4.93 g cm^{-3}. The density of TiC preforms was measured by Archimedes method in mercury.

Indirect upward infiltration process, which had proven feasible and reliable for fabricating dense and defect-free composites in the CoSi/SiC system[11] and NiAl/TiC system[6] in the previous group works of the authors, was also used in the present study and is schematically illustrated in Fig. 1. As-pressed TiC with relative density of 60% was used as feeder. The amounts of Fe28Al used for the infiltrations ranged from 85 to 140% of the total pore volumes of the TiC preform and the feeder. Fabrication steps used to prepare the composites are given in Table 1. The heating and cooling rates used for infiltrations were 25 and 10 °C min^{-1}, respectively.

Bars for the flexural strength tests were cut using a electro-discharge machine from the Fe28Al/TiC composite billets, further ground and polished to the final dimensions of 3 mm × 4 mm × 35 mm. Flexural strength samples with two levels of surface roughness were prepared by grinding on a (64 μm) diamond plated wheel and by polishing with 1 μm diamond paste, respectively, to study the effect of the surface roughness on the flexure strength. All samples were edge chamfered prior to flexural testing. Young's modulus of the composites was measured in the flexural test bars by the impulse excitation technique (GrindoSonic MK5, Belgium), the value of 0.2 being assumed for the Poisson ratio of all samples. Flexural strength was measured with a four-point bending rig of inner/outer spans of 10 mm/25 mm at a cross-head speed of 0.5 mm min^{-1}. Hardness of the composites was measured on fractured samples of the flexural strength tests by using a diamond Vickers indenter with normal loads of 98, 294 and 540 N and a dwell time of 15 s. Indentation crack sizes were measured by optical microscopy (Zeiss, Jenaphot 2000, Germany) with the quantitative image analysis software Quantimet500+. Indentation fracture (IF) toughness was determined from the equations proposed by Anstis et al.,[12] Niihara et al., [13] and Evans et al.[14] Each value of Vickers hardness and IF toughness was the average of at least five indentation tests on the sample.

Table 1
Fabrication techniques of Fe28Al/TiC composites

Fabrication techniques	Pre-sintering of TiC preform	Infiltration time and temperature	Amount of Fe28Al used for infiltration
No. 1	1500 °C × 4 h	1480 °C × 40 min	Equal to pore volume of TiC preform and feeder
No. 2	1500 °C × 1 h	1480 °C × 40 min	85% of pore volume of TiC preform and feeder
No. 3	1500 °C × 1 h	1480 °C × 40 min	Equal to pore volume of TiC preform and feeder
No. 4	1500 °C × 1 h	1580 °C × 40 min	Equal to pore volume of TiC preform and feeder
No. 5	1500 °C × 1 h	1480 °C × 40 min	140% of pore volume of TiC preform and feeder

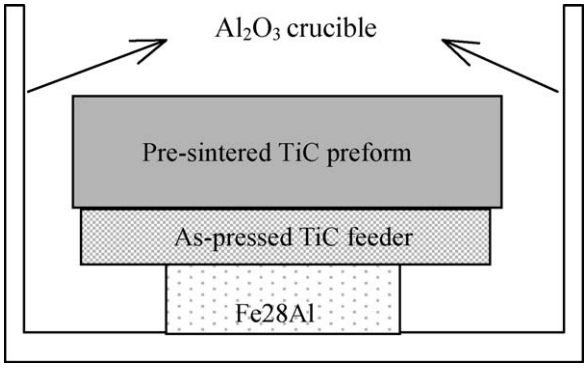

Fig. 1. Scheme of indirect upward infiltration.

The TiC volume fraction (V_{TiC}) of the composite was obtained from the density of the flexural test sample measured by Archimedes method in ethylenglycol ($d_{measured}$), by applying the following equation:

$$6.60 \times 0.995(1 - V_{TiC}) + 4.93 \times 0.995\, V_{TiC} = d_{measured} \quad (1)$$

where the residual porosity of the composites of 0.5% is assumed, and 6.60 and 4.93 g cm^{-3} are the theoretical density of Fe28Al and TiC, respectively.

The microstructure and fracture surfaces of the composites were observed by scanning electron microscope (SEM, Hitachi, S-4100, Japan). Solubility of Ti in the intermetallic phase and Fe and Al in the TiC grains was determined by EDS (Rontec) in transmission electron microscopy (TEM, Hitachi, H-9000NA,

Japan). Crystalline phases of the composites were identified by X-ray diffraction (XRD, Rigaku, Geigerflex/D).

3. Results and discussions

3.1. Microstructural evolution during infiltration

For the amount of molten Fe28Al ranging from 85 to 140% of the total pore volume of the TiC preform and the feeder, the infiltration was complete under the conditions listed in Table 1. From the SEM observations of the microstructures, the composites were nearly with no obvious pores or voids. TiC and Fe28Al were properly bound. Infiltration of Fe28Al in porous TiC preforms was adequate to produce a fully dense and defect-free microstructure even though the preforms had a relative density as high as 88–89% of the theoretical density of TiC (Table 1, No. 1), or the amount of Fe28Al used for infiltration was at first seen as insufficient to occupy the original pore volume of the TiC preform and the feeder (Table 1, No. 2). TiC particles were further liquid sintered and re-arranged during the infiltration process. The composites shrunk or expanded during infiltration to accommodate the insufficient (e.g., Table 1, No. 2) or excessive (e.g., Table 1, No. 5) volume of Fe28Al, leading to dense microstructures in both cases.

Fig. 2(a) and (b) are representative SEM micrographs of the composites with 90 vol.% TiC and 75 vol.% TiC, for which the infiltrated Fe28Al amounts were 100 and 140% of the total pore volume of the initial pre-sintered preform and as-pressed feeder, respectively (Table 1, No. 1 and No. 5). The dark grains in Fig. 2 are TiC and the gray phase is Fe28Al. XRD analysis confirmed that the composites have only the original crystalline phases of Fe_3Al and TiC. Comparing the microstructure of the composites (e.g., Fig. 2(a) and (b)) with those of the corresponding TiC preforms used (1500 °C × 4 h and 1500 °C × 1 h pre-sintered, Fig. 3(a) and (b)), it is found that direct bonding of TiC grains from the previous solid-state pre-sintering step was preserved in most of the composites with high TiC content (e.g., Fig. 2(a)). However, many of the initially connected TiC particles were separated into individual particles in composites with high intermetallic content (e.g., Fig. 2(b)). EDS analysis in TEM showed that there is about 1–2 at.% Ti dissolved in Fe28Al and there are also Fe and Al traces in the outer layer of the TiC grains. Molten Fe28Al not only filled the existing void channels of the TiC preform, but also corroded and permeated many grain boundaries of the bonded TiC particles in a multi-step mechanism of dissolution/reaction infiltration. The dissolution of TiC in the intermetallic phase favors wetting and infiltration.

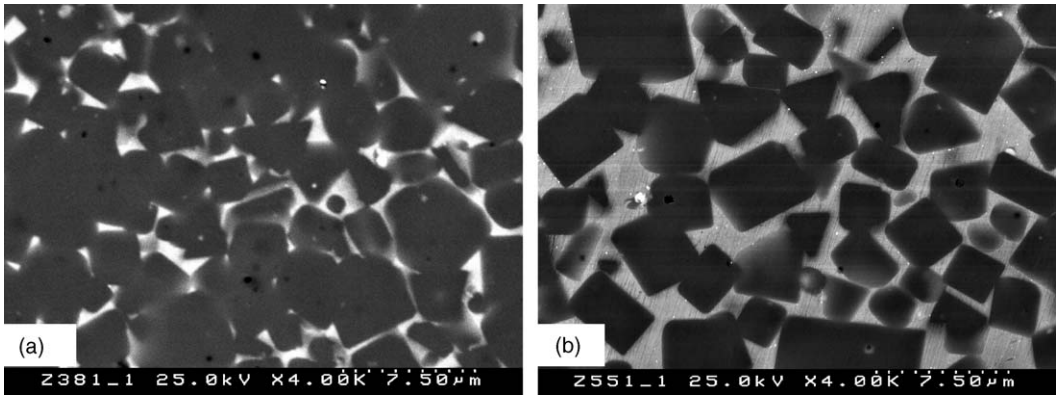

Fig. 2. SEM micrographs of Fe28Al/TiC composites: (a) 90 vol.% TiC, infiltrated from 1500 °C × 4 h pre-sintered TiC preform, amount of Fe28Al infiltrated equal to pore volume of preform and feeder; (b) 75 vol.% TiC, infiltrated from 1500 °C × 1 h pre-sintered TiC preform, amount of Fe28Al infiltrated equal to 140% pore volume of preform and feeder.

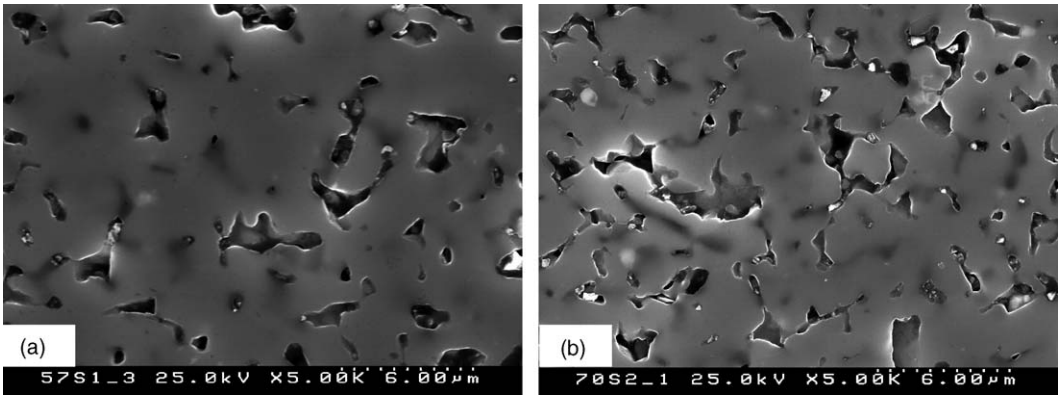

Fig. 3. SEM micrographs of pre-sintered TiC preforms: (a) 1500 °C × 4 h pre-sintered; (b) 1500 °C × 1 h pre-sintered.

Table 2
Flexural strength (σ_b), Vickers hardness (H_v), indentation fracture toughness ($K_{c(Anstis)}$), Weibull modulus and Young's modulus (E) of Fe28Al/TiC fabricated by different techniques

Fabrication techniques	Vol.% TiC	σ_b (MPa)	H_v (GPa)	$K_{c(Anstis)}$ (MPa m$^{1/2}$)	Weibull modulus	E (GPa)
No. 1 (17 bars)	90 ± 1.2	990 ± 90	15.5 ± 0.5	6.5 ± 0.5	13	400 ± 15
No. 2 (6 bars)	87.3 ± 1.3	1060 ± 70	14.6 ± 0.6	7.6 ± 0.3	16	390 ± 15
No. 3 (15 bars)	83.6 ± 1.1	1110 ± 80	12.0 ± 0.8	10.1 ± 0.7	17	370 ± 10
No. 4 (14 bars)	81.6 ± 1.5	1220 ± 70	11.3 ± 0.8	11.2 ± 0.5	20	360 ± 10
No. 5 (11 bars)	77.0 ± 3.0	1260 ± 80	10.6 ± 0.8	12.0 ± 0.7	19	340 ± 10

3.2. Mechanical properties of the composites

The mechanical properties including Young's modulus, flexural strength, Weibull modulus, Vickers hardness and IF toughness of the composites obtained by the Anstis equation under a load of 98 N for given TiC fractions are summarized in Table 2. There is a small gradient of Fe28Al content from the bottom to the top of the infiltrated billets. The TiC content at the topside is 2–4 vol.% higher than that at the bottom. Higher infiltration temperature (1580 °C) led to a more sufficient infiltration than lower infiltration temperature (1480 °C), yielding a composite with higher Fe28Al volume fraction, as more intermetallic infiltrated from the feeder to the preform (Tables 1 and 2, comparing No. 3 to No. 4). Young's modulus (E) of the composites is a TiC content dependent property, as seen in Table 2, it increases with increasing TiC content. The measured values of E are very close to those predicted by the Ravichandran equation,[15] in which the Young's modulus of Fe28Al and TiC of 140 and 430 GPa, respectively, were adopted.

For every single bar cut from the same billet, the flexural strength was not simply influenced by the TiC content gradient pointed out above, but also by micro-pores and residual stresses caused by thermal mismatch. Yet, the average value of flexural strength increases with increasing intermetallic content as shown in Table 2. The Weibull modulus of the strength distribution of the composites, estimated as reported by Plucknett et al.,[4] is also given in Table 2. The scatter of strength values of Fe28Al/TiC is low. Unlike the case of high strength ceramics,[16] the flexural strength of Fe28Al/TiC composites in the present study was not consistently lowered by coarse surface finishing. It is so at least in the range of from 1 μm polishing to the 64 μm abrasive grinding. It is worthwhile to emphasize that economical surface finishing can be safely done by using the coarse abrasives, at least up to 64 μm particle size in this material. The strength of Fe28Al/TiC composites is 30 to 60% higher than the strength of Fe40Al/TiC composites with the same TiC content reported by Subramaniam et al.,[2,3] despite the fact that four-point bending strength tests (present study) usually give lower values of strength than the three-point bending strength tests (in the literature[2,3]). Although there is a high strength range in Ni_3Al/75–80 vol.% TiC composites, of 1270 to 1070 MPa, as reported by Plucknett et al.,[4] however, a considerable low strength range (640 MPa) also existed in the same composites. The values of average strength of samples in Table 2 exceed by 100–200 MPa the strength of Ni_3Al/TiC composites with equal TiC contents (75–85 vol.%),[4] but are much higher than 670 MPa, the average strength of NiAl/86 vol.% TiC composites.[6]

The high flexural strength of the Fe28Al/TiC composites is attributed to the processing optimization coupled to the high values of fracture energy of the composites. Pores with sizes of 15–30 μm were frequently found in the composites of first trial experiments, which originated from voids in the TiC preform caused by agglomerates. The capillary force in the large pores is not enough to sustain molten intermetallic infiltration with equal speed throughout the sample. Those large pores were eliminated by milling the as-received TiC powder as described above. Instead of using as-pressed TiC preforms as in most early studies,[2–5] pre-sintered TiC preforms with controlled porosity were used for infiltration in the present study. Pre-sintering led to less re-arrangement of TiC grains and less shrinkage of the spaces in between them during infiltration, especially when composites of high TiC content are intended. The relative density of Ni_3Al/TiC with 10–15 vol.% of intermetallic was lower than 96–98% of the theoretical density of the composite when as-pressed preforms were directly used.[4] The same difficulty in attaining full dense Fe40Al/TiC composites by melt infiltration, especially when the content of Fe40Al was lower than 20 vol.%, is also reported by Subramaniam et al.[3] But all Fe28Al/TiC composites with TiC content ranging 75–90 vol.% in present study have nearly theoretical density. Pre-sintering also imparted high strength to the preforms and minimized the deformation under the melt surface tension, especially when large-sized preforms were infiltrated. Thus, crack-like pores caused by deformation, which were often found with as-pressed TiC preforms were avoided. In the indirect infiltration process, the molten Fe28Al first infiltrated the feeder, coating and covering of the preform surfaces by the melt being restrained. The risk of sealing gases inside the preform and leaving closed pores behind was diminished. These changes of the fabrication process all favored the densification of the composites, with the dense and nearly defect-free microstructures guaranteeing high strength and high Weibull modulus.

The average values of Vickers hardness (H_v) and of IF toughness as determined by the Anstis equation of the composites fabricated by different infiltration technique for the indentation load of 98 N are given in Table 2. Vickers hardness has a nearly linear increase with the TiC content of the composites. Values of Vickers hardness are also close to that of Ni_3Al/80–88 vol.% TiC as reported by Plucknett et al.[4] The dependence of the IF toughness of the individual tested samples under a load of 98 N as assessed by different equations on TiC volume fraction is plotted in Fig. 4. At 98 N normal load the relative indentation crack size of samples with TiC content below 76 vol.% do not fulfill the criterion of crack-to-indent ratio ($3.5 > c/a > 1.25$) for

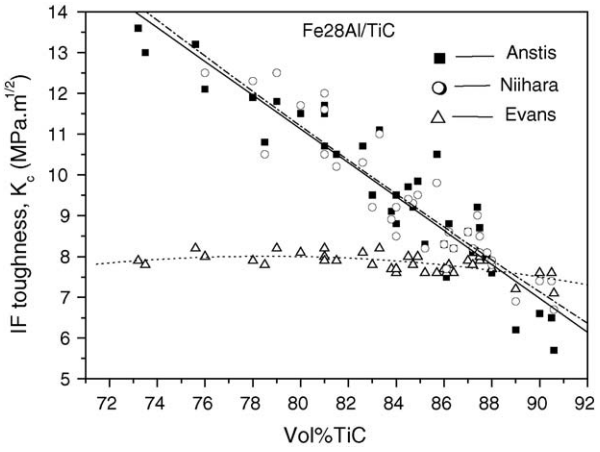

Fig. 4. The dependence of Vickers hardness, IF toughness (assessed by different equations) on TiC content of Fe28Al/TiC (indentation load of 98 N).

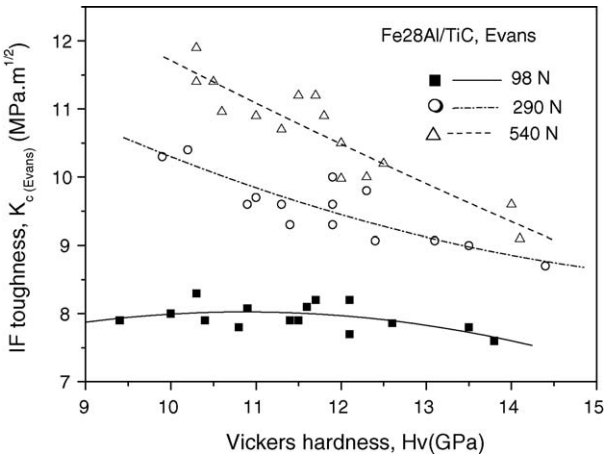

Fig. 6. Variations of the Evans IF toughness of Fe28Al/TiC under different indentation load.

applying Niihara's IF toughness (c being the indentation crack size and $2a$ being the indent diagonal).[13] The Niihara equation for IF toughness is not applied to those samples. The IF toughness at 98 N determined by the Anstis[12] and Niihara[13] equations is strongly correlated with TiC content. For TiC content ranging 76–88 vol.%, Niihara and Anstis IF toughness values display a similar correlation to TiC content. The Anstis and Niihara IF toughness data in Fig. 4 closely match, at lower values of K_c (<13 MPa m$^{1/2}$), the dependence of the long-crack fracture toughness of Fe40Al/TiC cermets and of commercially available Ni-16Mo cermets determined with Chevron-notched beams in three-point bending tests.[3]

The dependence of Anstis IF toughness on H_v for normal loads of 98 N is approximated to a linear relationship and fits the following equation as summarized from Fig. 5:

$$K_{c(\text{Anstis})} = 22.3 - 1.0H_v \quad (2)$$

This relationship is useful in predicting the direction of changes of hardness and fracture toughness of the composites for engineering applications. For Vickers hardness ranging over 10.0–14.5 GPa (corresponding TiC content 76–88 vol.%), the dependence of Niihara IF toughness on H_v is very similar to that of Anstis, but Niihara values are a little higher than Anstis values out of this range (Fig. 5).

However, the IF toughness assessed by using the Evans equation[14] at 98 N is weakly correlated to TiC content (Fig. 4) and also to H_v (Fig. 5). The Evans equation of micro-toughness applies a polynomial function of (c/a) with empirical coefficients to determine the micro-toughness of brittle materials. The effect of indentation normal load on the values of IF toughness determined by applying the Evans equation is further investigated in Fig. 6. The values of IF toughness determined by the Evans equation at the highest normal load of 540 N also reveal the strong dependence of IF toughness on Vickers hardness of the composites.

3.3. Fracture mechanism of the composites

Fig. 7 shows the fracture surfaces of Fe28Al/TiC. TiC grains fractured by cleavage. Although bulk iron aluminides and other intermetallics are brittle at room temperature,[8,17] Fig. 7 shows significant plastic strains from the ductile behaviour of Fe28Al

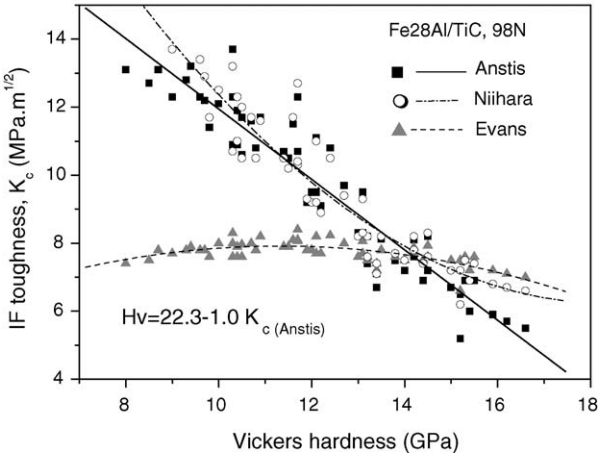

Fig. 5. Relations of Vickers hardness and IF toughness of Fe28Al/TiC assessed by different equations under a load of 98 N.

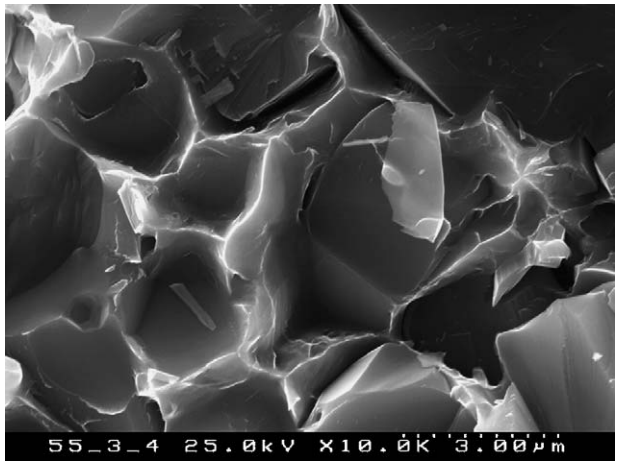

Fig. 7. A representative SEM micrograph of the fracture surfaces of Fe28Al/TiC (75 vol.% TiC).

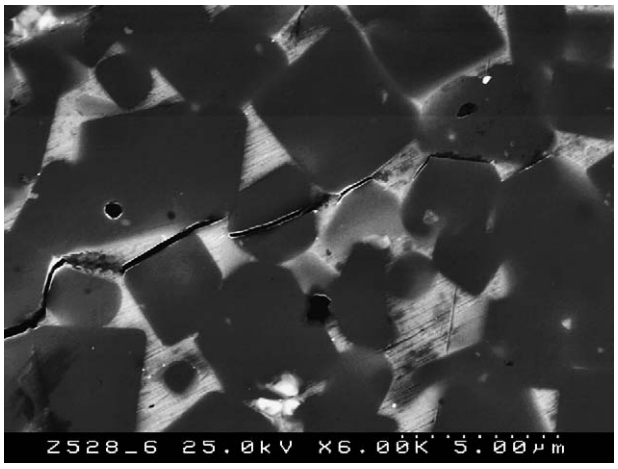

Fig. 8. SEM micrograph of an indentation crack under a load of 98 N.

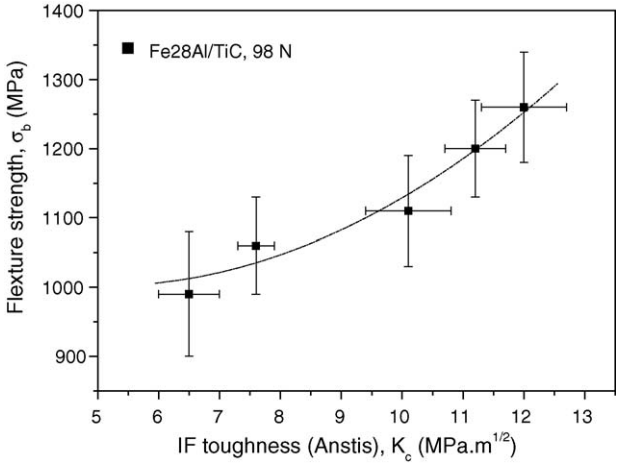

Fig. 9. The dependence of the average four-point bending strength of Fe28Al/TiC on the IF toughness assessed by the Anstis equation under a load of 98 N.

phase in the composites. The grain growth during solidification of the Fe28Al phase yields very large grain size (≫10 μm). The strained intermetallic bridges are single crystal domains with large ultimate fracture strain. Bridging zone lengths in excess of 100 μm and blunting of the crack profile in Ni_3Al/TiC composites at room temperature were also reported.[18]

De-bonding of the Fe28Al and TiC grain interfaces was frequently found on the fracture surface in SEM. As seen in Fig. 7, concavities of the fracture surface expose places where TiC was pulled-out. Bridging by the intermetallic ligaments and by dislodged and rotated lumps of TiC grains screens the applied stress and reduces the crack tip stress concentration, thus increasing the fracture resistance. Fig. 8 shows the indentation crack tip on the surface for the normal load of 98 N. Crack deflection along the Fe28Al/TiC interface and through cleavage planes of TiC grains is observed. That fracture initially occurred in both the interface between Fe28Al and TiC grains and through TiC grains implies that the interface strength and the TiC cleavage strength are at same level. By accounting for the work deformation of the metallic phase, crack deflection brings a minor contribution to the toughness for the samples with high Fe28Al volume fraction. The plastic deformation of the Fe28Al ligaments is noticeably seen bridging the crack walls, again implying a ductile toughening behaviour of the thin Fe28Al ligaments in the composite structure rather than brittle cleavage, which is hardly envisaged in the room temperature fracture of the bulk Fe28Al itself.

The dependence of the average four-point bending strength on the IF toughness of the Fe28Al/TiC composites given in Table 2 is plotted in Fig. 9. A strong increase of strength is observed in proportion with the increase of toughness with volume fraction of the intermetallic reinforcement in the structure of the composite. As it is shown in Fig. 10, the high values of fracture energy also increase the mechanical reliability, the Weibull modulus being linearly correlated to the values of the IF toughness. Large bridging zone lengths from the ultimate strain of the single crystal Fe28Al ligaments would imply raising R-curve behaviour for the dependence of fracture energy on crack extension.[19] Depending on the critical crack sizes for fracture initiation and for values of these below the bridging zone length the raising R-curve of toughness will improve the fracture strength at the same time as the mechanical reliability as measured by the Weibull modulus, *m*.

Indentation tests would only reveal the full values of fracture toughness if the applied normal load creates indentation cracks of size (*c*) well above the bridging zone length of the toughened material. With high normal loads, interfering lateral cracks may appear. There is a normal load effect on the values of IF toughness of Fe28Al/TiC (Fig. 6). Values of fracture toughness measured by indentation are underestimates of the dependence of K_c on the volume fraction of toughening particles and ligaments structures that is better assessed by the flexural testing of notched beams,[20] as it is known for the Fe40Al/TiC,[2,3] Ni_3Al/TiC[4] and Ni_3Al/Al_2O_3[21] composites. Nevertheless, from the values in Fig. 4, IF toughness of the composites even with TiC content as high as 90 vol.% remains well above that of TiC ceramics, which is only 1.5–3.6 MPa m$^{1/2}$ when also assessed with the Anstis equation.[1] Accordingly to Ashby et al.,[22] weak interfacial bonding results in high energy absorption in fracture and, therefore, in high fracture toughness. Furthermore,

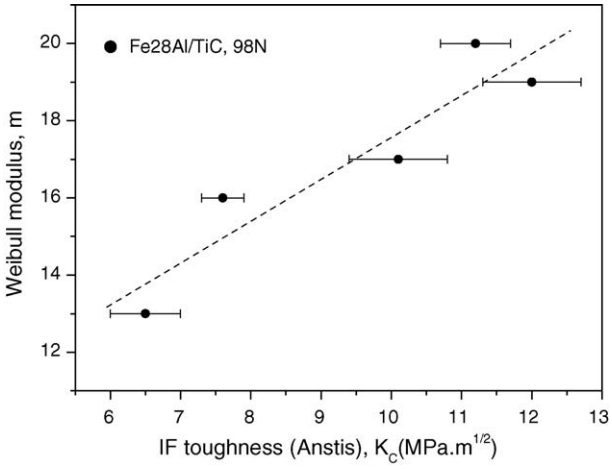

Fig. 10. The relationship between flexure Weibull modulus and the IF toughness assessed by the Anstis equation under a load of 98 N.

the high density of interpenetrated networks of Fe28Al ligaments in the TiC structure of the composites also favors the large fracture toughness as reported in different ceramic matrix composites.[23,24]

Strong toughening effect has been achieved in the composites by the strengthening effect of the Fe28Al ligaments. Small surface flaws, grooves and surface damage are screened by crack blunting and the raising R-curve behaviour of toughness coming from plastic strain of the intermetallic phase. The effect is intensified by the large ultimate strain of the single crystal domains of the plastic phase. The fracture energy is dissipated as much as the plastic deformation of Fe28Al phase is promoted by the TiC hard particle skeleton of the melt infiltrated cermets.

4. Conclusions

At the temperature of 1480 and 1580 °C in the upward indirect infiltration process, Fe28Al melt can spontaneously infiltrate TiC preforms with relative density of up to 80–88% obtained by pre-sintering. The infiltration of Fe28Al into porous TiC preforms was always adequate whether the amount of Fe28Al used for infiltration was insufficient or excessive to fill the pore volume of TiC preform and TiC feeder. The TiC grains rearranged, the spaces among the TiC grains shrunk or expanded during infiltration depending on the amount of Fe28Al used, but all led to nearly defect-free and dense microstructures. The flexural strength of Fe28Al/TiC with TiC content of 76 ± 3 to 90 ± 1.2 vol.% ranges from 1260 ± 80 to 990 ± 90 MPa, the corresponding Vickers hardness ranges from 10.6 ± 0.8 to 15.7 ± 0.5 GPa. Vickers hardness increases but fracture toughness decreases with increasing TiC volume fraction. Vickers hardness and indentation fracture toughness display linear relationship given by the power equation, $K_{c(\text{Anstis})} = 22.3 - 1.0H_v$. The thin Fe28Al ligaments filling the TiC intergranular spaces show a ductile behaviour, bridging the cleaved cracks within the TiC grains during the fracture process.

Acknowledgements

This work is sponsored by National Natural Science Foundation of China (Grant No. 50272060) and by GRICES-The Institute of International Science and Technology Cooperation of MCEIS Portugal (4.1./China/am) and Ministry of Science and Technology, PR China.

References

1. Maerky, C., Guillou, M. O., Henshall, J. L. and Hooper, R. M., Indentation hardness and fracture toughness in single crystal $TiC_{0.96}$. *Mater. Sci. Eng.*, 1996, **A209**, 329–336.
2. Subramaniam, R., Schneibel, J. H., Alexander, K. B. and Plucknett, K. P., Iron-aluminide-titanium carbide composites by pressurless melt infiltration—microstructure and mechanical properties. *Scripta Materialia*, 1996, **35**(5), 583–588.
3. Subramaniam, R. and Schneibel, J. H., FeAl-TiC and FeAl-WC composites—melt infiltration processing, microstructure and mechanical properties. *Mater. Sci. Eng.*, 1998, **A244**, 103–122.
4. Plucknett, K. P., Becher, P. F. and Waters, S. B., Flexural strength of melt-infiltration-proceed titanium carbide/nickel aluminide composites. *J. Am. Ceramic Soc.*, 1998, **81**(7), 1839–1844.
5. Pan, Y. and Sun, K. W., Preparation of TiC/Ni_3Al composites by upward melt infiltration. *J. Mater. Sci. Tehnol.*, 2000, **16**(4), 387–392.
6. Gao, M. X., Pan, Y., Oliveira, F. J., Baptista, J. L. and Vieira, J. M., Interpenetrating microstructure and fracture mechanism of NiAl/TiC composites by pressureless melt infiltration. *Mater. Lett.*, 2004, **58**, 1760–1765.
7. Durlu, N., Titanium carbide based composites for high temperature application. *J. Eur. Ceram. Soc.*, 1999, **19**(13–14), 2415–2419.
8. Liu, C. T., Mckamey, C. G. and Lee, E. H., Environment effect on room temperature ductility and fracture in Fe_3Al. *Scripta Metall. Mater.*, 1990, **24**(2), 385–390.
9. Mckamey, C. G., DeVan, J. H., Tortorelli, P. F. and Sikka, V. K., A review of recent developments in Fe_3Al-based alloys. *J. Mater. Res.*, 1991, **6**(8), 1779–1805.
10. Hawk, J. A. and Alman, D. E., Abrasive wear of intermetallic-based alloys and composites. *Mater. Sci. Eng.*, 1997, **A240**, 899–906.
11. Pan, Y., Yi, X. S. and Baptista, J. L., Kinetic study of cobalt silicide infiltration into silicon carbide preforms. *J. Am. Ceram. Soc.*, 1999, **82**(12), 3459–3465.
12. Anstis, G. R., Chantikul, P., Lawn, B. R. and Marshall, D. B., A critical evaluation of indentation techniques for measuring fracture toughness. I. Direct crack measurements. *J. Am. Ceram. Soc.*, 1981, **64**(2), 533–538.
13. Niihara, K., Morena, R. and Hasselman, D. P. H., Evaluation of K_{Ic} of brittle solids by the indentation method with low crack to indent ratios. *J. Mater. Sci. Lett.*, 1982, **1**, 13–16.
14. Evans, A. G., In *Fracture Mechanic Applied to Brittle Materials*, ed. S. W. Freiman. American Society for Testing and Materials, Philadelphia, 1979, pp. 112–135, part 2.
15. Ravichandran, K. S., A simple model of deformation behaviour of two phases composites. *Acta Metall. Mater.*, 1994, **42**(4), 1113–1123.
16. Zheng, Y. S., Vieira, J. M., Oliveira, F. J., Davim, J. P. and Brogueira, P., Relationship between flexural strength and surface roughness for hot-pressed Si_3N_4 self-reinforced ceramics. *J. Eur. Ceram. Soc.*, 2000, **20**(9), 1345–1353.
17. Liu, C. T., Lee, E. H. and Mckamey, C. G., An environment effect as the major cause for room-temperature embrittlement in FeAl. *Scripta Metall.*, 1989, **23**(5), 875–880.
18. Becher, P. F., Plucknett, K. P. and Hsueh, C. H., Toughening and strengthening response in Ni_3Al-bonded titanium carbide cermets. *Zeitschrift fur Metallkun*, 2001, **92**(8), 995–999.
19. Li, C.-W. and Yamanis, J., Super-tough silicon nitride with R-curve behaviour. *Ceram. Eng. Sci. Proc.*, 1989, **10**(7–8), 632–645.
20. Muscat, D., Harris, R. L. and Draw, R. A. L., The effect of pore size on the infiltration kinetics of aluminium in titanium carbide preform. *Acta Metall. Mater.*, 1994, **42**(12), 4155–4163.
21. Sglavo, V. M., Marino, F., Zhang, B. R. and Gialanella, S., Ni_3Al intermetallic compound as second phase in Al_2O_3 ceramic composites. *Mater. Sci. Eng.*, 1997, **A239–240**, 665–671.
22. Ashby, M. F., Blunt, F. J. and Bannstier, M., Flow characteristics of highly constrained metal wires. *Acta Metall.*, 1989, **37**(7), 1847–1857.
23. Rödel, J., Prielipp, H., Claussen, N., Sternitzke, M., Alexander, K. B. and Becher, P. F., Schneibel, Ni_3Al/Al_2O_3 composites with interpenetrating networks. *Scripta Metall. Mater.*, 1995, **33**(5), 843–848.
24. Klassen, T., Gunther, R., Dickau, B., Gartner, F., Bartels, A., Bormanm, R. *et al.*, Processing and properties of intermetallic/ceramic composites with interpenetrating microstructure. *J. Am. Ceram. Soc.*, 1998, **81**(9), 2504–2506.